

The logo for EPJ B consists of a dark blue rectangle with a red and orange abstract pattern on the left side. The text "EPJ B" is written in a white, serif font in the center of the blue area.

*EPJ B*

[www.epj.org](http://www.epj.org)

Condensed Matter  
and Complex Systems

Eur. Phys. J. B **67**, 251–257 (2009)

DOI: 10.1140/epjb/e2009-00022-x

## **A data-analysis method for decomposing synchronization variability of anticipatory systems into stochastic and deterministic components**

N. Stepp and T.D. Frank



## A data-analysis method for decomposing synchronization variability of anticipatory systems into stochastic and deterministic components

N. Stepp<sup>1,2,a</sup> and T.D. Frank<sup>1</sup>

<sup>1</sup> Center for the Ecological Study of Perception and Action, University of Connecticut, 406 Babbidge Road, Storrs, CT 06269, USA

<sup>2</sup> Haskins Laboratories, 300 George St, New Haven, CT, USA

Received 20 October 2008

Published online 22 January 2009 – © EDP Sciences, Società Italiana di Fisica, Springer-Verlag 2009

**Abstract.** Synchronization has been shown to be a valuable concept in the field of nonlinear dynamics and dynamical systems in general. Deviation from perfect synchronization results from an interplay of deterministic coupling forces and stochastic fluctuating forces. When the exact details of these two sources of variance are unknown, it becomes useful to estimate them directly from data. To this end, we develop a data analysis method for estimating parameters associated with these deterministic and stochastic components. The method relies on separating their respective contributions to synchronization error. We focus on the case where a slave system synchronizes with the future of a master system, so-called anticipatory synchronization.

**PACS.** 02.30.Ks Delay and functional equations – 05.45.Tp Time series analysis

### 1 Introduction

When two dynamical systems  $x$  and  $y$  are coupled, it becomes possible for those systems to synchronize [1]. One particular form of synchronization requires that the difference between states of the two systems is minimized. The difference between the states  $x(t)$  and  $y(t)$  may be zero just in case the two systems are exactly synchronous in time. It is also possible that this difference deviates from zero while the difference between  $x(t - \tau)$  and  $y(t)$  or the difference between  $x(t)$  and  $y(t - \tau)$  become zero, where  $\tau$  denotes a synchronization lag. Taking the signal  $x(t)$  as our reference point in the former case we are dealing with lagged synchronization, whereas in the latter case we have anticipatory synchronization.

Synchronization (whether ordinary, lagged or anticipatory) plays an important role in human-machine interactions and master-slave systems in general [2,3]. The synchronization error between master and slave depends on the coupling between them and the perturbations to which the slave is subjected. In particular, the variability of the synchronization crucially depends on master-slave coupling on the one hand and the coupling of the slave to noise sources on the other hand [4]. Figure 1 illustrates this issue.

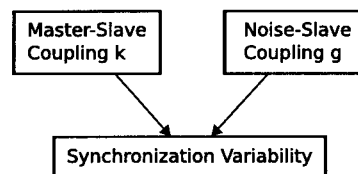


**Fig. 1.** Sources of synchronization variability. Synchronization variability, or synchronization error, has two major contributing components: variability is increased due to stochastic forces resulting from slave-noise process coupling, and decreased due to deterministic forces resulting from master-slave coupling.

In the case of a master-slave that involves a unidirectional coupling between master and slave – as shown in Figure 2 – the two key parameters that are essential for our understanding of the synchronization error and the synchronization variability are the master-slave coupling constant  $k$  and the constant  $g$  describing to what extent the slave is affected by noise sources. The objective of our study is to show how  $k$  and  $g$  can be estimated from time series data in the case of master-slave systems that show the aforementioned anticipatory synchronization. In fact, several recent studies [5–9], centered around a data analysis method proposed by Friedrich and Peinke [10], have been devoted to reconstructing from time

<sup>a</sup> e-mail: nigel.stepp@uconn.edu

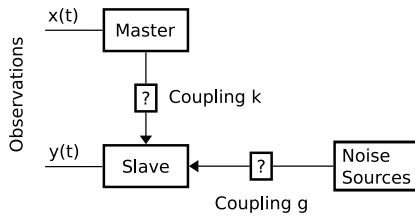


**Fig. 2.** Master-slave-noise coupling arrangement. Master-slave coupling parameter  $k$  and slave-noise coupling parameter  $g$  are shown here in their relative arrangement around the slave.

series, deterministic and stochastic components, here  $k$  and  $g$ . While ordinary and lagged synchronization have been studied in this context [11,12], the anticipatory case has not yet been addressed.

Synchronization in anticipatory systems, where the evolution of the slave precedes that of the master, has been examined in several previous studies [13–15]. The general form for one case of *anticipating synchronization* is

$$\begin{aligned} \frac{d}{dt}\mathbf{x} &= f(\mathbf{x}) \\ \frac{d}{dt}\mathbf{y} &= f(\mathbf{y}) + k(\mathbf{x} - \mathbf{y}_\tau) \end{aligned} \quad (1)$$

where  $\mathbf{y}_\tau$  is defined to be  $\mathbf{y}(t - \tau)$ . In the synchronized state,  $\mathbf{y}(t)$  corresponds to  $\mathbf{x}(t + \tau)$  – the slave anticipating<sup>1</sup> the master.

In general, however, synchronization of anticipatory systems exhibits variability. That is, on average, the state of the slave at time  $t$  corresponds to the state of the master at time  $t + \tau$ , but at particular points in time the two states will differ by some amount. We will refer to this difference as the synchronization error. The variability of synchronization error has been investigated in both simulated and physical systems [4,15,16].

In equation (1) we laid out the general form for systems which exhibit anticipating synchronization. As noted, however, in general we expect a stochastic component. Therefore, a more correct system of study has the form

$$\begin{aligned} \frac{d}{dt}\mathbf{x} &= \mathbf{f}(\mathbf{x}) \\ \frac{d}{dt}\mathbf{y} &= \mathbf{f}(\mathbf{y}) + k(\mathbf{x} - \mathbf{y}_\tau) + g\mathbf{\Gamma} \end{aligned} \quad (2)$$

where  $\mathbf{x}, \mathbf{y}$  are  $L$ -dimensional state vectors (i.e. we have  $\mathbf{x} = (x_1, \dots, x_L)$ ,  $\mathbf{y} = (y_1, \dots, y_L)$ ,  $\mathbf{f}$  is a function,  $k$  a coupling matrix,  $\mathbf{\Gamma}$  is a normalized fluctuating force, and  $g$  is a matrix of noise amplitudes. Finally,  $\tau$  denotes a delay, such that  $\mathbf{y}_\tau(t) = \mathbf{y}(t - \tau)$ .

Synchronization error, then, results from an interplay between both the coupling force between master and slave

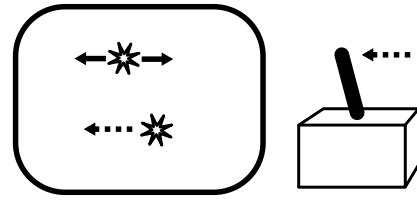


**Fig. 3.** Anticipatory Synchronization Task. A dot oscillates at the top of a screen (solid arrows). A joystick controls the motion of a second dot at the bottom of the same screen (dashed arrows). The task consists of synchronizing the motion of the two dots by manipulating the joystick. If the effect of the joystick is delayed, however, then the oscillating dot must be anticipated for synchronization to take place.

and the fluctuating force acting only on the slave (see Fig. 1). In general, the error increases when the strength of the coupling force decreases. Likewise, the error increases when the strength of the fluctuating force increases. In other words, the degree of synchronization variability is determined by the strength of the master-slave coupling and the strength of the fluctuating force acting on the slave.

Therefore, the question arises: how can we quantify the impacts of these two forces? In Section 2 we will develop a time series analysis method that can be used to determine simultaneously from a given data set the strength of the coupling force between master and slave and the amplitude of the fluctuating force that acts on the slave. Our proposed data analysis methods will be applied to systems subjected to both natural boundary conditions and periodic boundary conditions.

Being able to determine these parameters can be useful for characterizing empirical data where the coupling strength (or mechanism) is not obvious. Consider, for example, an experimental setup such as the one described in Figure 3. The figure shows a typical example of a human operator interacting with a machine using a tool. In this example, the tool is a joystick, which the human operator uses to control an indicator on a display. The situation described here parallels the general dynamics of equation (2), however the values of  $k$  and  $g$  remain elusive. The data analysis method presented here provides a systematic way to determine the values of  $k$  and  $g$  from collected data.

## 2 Data analysis method

Assuming collected time series data has been produced according to equation (2), our task is to estimate  $k$  and  $g$ . We may work in time-discrete terms and assume that we have experimental observations  $\mathbf{x}_n, \mathbf{y}_n$  with a sampling interval  $\Delta$ . In this case, the time-discrete evolution is approximately given by

$$\begin{aligned} \mathbf{x}_{n+1} &= \mathbf{x}_n + \Delta\mathbf{f}(\mathbf{x}) \\ \mathbf{y}_{n+1} &= \mathbf{y}_n + \Delta\{\mathbf{f}(\mathbf{y}) + k(\mathbf{x}_n - \mathbf{y}_{n-m})\} + g\mathbf{w}_n \end{aligned} \quad (3)$$

<sup>1</sup> In the context of human-machine interactions, anticipation is taken to be approximation of some future behavior, for instance by maintaining a negative phase relationship.

where  $\mathbf{w}_n$  is a time-discrete fluctuating force that will be approximated by Gaussian random numbers with variance  $\Delta$  (i.e. by the increment of a multivariate Wiener process with variance  $n\Delta t$ ). And  $\tau = m\Delta$ . At issue is to determine  $m$ ,  $k$ , and  $g$  from experimental data  $\mathbf{x}_n$ ,  $\mathbf{y}_n$  given that the function  $\mathbf{f}$  and the sampling interval  $\Delta$  are known.

The magnitude of the delay,  $m$ , can be estimated if we make the assumption that our data has reached a steady-state of synchronization. If this is the case, the cross correlation of master and slave will be maximized at lag  $m$ , i.e.

$$\text{cov}_{\mathbf{x},\mathbf{y}}(m) = \max(\text{cov}_{\mathbf{x},\mathbf{y}}(\tau)) \tag{4}$$

for lags  $\tau$ . This estimation of  $m$  will be accurate as long as the mean synchronization error approaches zero.

The similarity function [17] provides a second method for the estimation of  $\tau$

$$S^2(\tau) = \frac{\langle [y(t+\tau) - x(t)]^2 \rangle}{[\langle x^2(t) \rangle \langle y^2(t) \rangle]^{1/2}}. \tag{5}$$

Similar in form to a covariance,  $S^2$  is tailored so that it is minimum for the appropriate  $\tau$ . In similar fashion then, we choose  $m$  so that

$$S^2(m) = \min(S^2(\tau)) \tag{6}$$

for lags  $\tau$ . Both methods should pick similar values for appropriate  $m$ .

Once the delay has been estimated, we turn to  $k$  and  $g$ . As a first step, we introduce

$$\mathbf{u}_n = \mathbf{y}_{n+1} - \mathbf{y}_n - \Delta \mathbf{f}(\mathbf{y}_n) \tag{7}$$

and

$$\mathbf{z}_n = \mathbf{x}_n - \mathbf{y}_{n-m}. \tag{8}$$

Then it follows that

$$\mathbf{u}_n = \Delta k \mathbf{z}_n + g \mathbf{w}_n. \tag{9}$$

We determine  $k$  from a linear regression analysis of  $\mathbf{u}_n$  with respect to  $\mathbf{z}_n$ . We assume that  $g$  is a diagonal matrix with diagonal elements  $g_{ii}$ . We determine the parameters  $g_{ii}$  by computing the average

$$g_{ii}^2 = \Delta^{-1} \langle (\mathbf{u}_n - \Delta k \mathbf{z}_n)_i^2 \rangle. \tag{10}$$

The linear coupling force in equation (2) can be regarded as the first expansion term of a Taylor expansion applied to a more general nonlinear coupling force. In line with this interpretation of the coupling force for a system subjected to natural boundary conditions, we consider systems subjected to periodic boundary conditions for which the coupling force is again given by the lowest nontrivial expansion term of an appropriate expansion. In the case of periodic systems, the expansion is a Fourier expansion and the lowest order term corresponds to a sine function.

Consequently, we consider next anticipatory systems subjected to periodic boundary conditions that assume the form

$$\begin{aligned} \frac{d}{dt} \mathbf{x} &= \mathbf{f}(\mathbf{x}) \\ \frac{d}{dt} \mathbf{y} &= \mathbf{f}(\mathbf{y}) + k \begin{pmatrix} \sin(x_1 - y_{1,\tau}) \\ \dots \\ \sin(x_L - y_{L,\tau}) \end{pmatrix} + g \mathbf{\Gamma}. \end{aligned} \tag{11}$$

The preceding analysis can be applied to this kind of system as well. To this end, we need to replace equation (8) by

$$\mathbf{z}_n = \begin{pmatrix} \sin(x_1 - y_{1,\tau}) \\ \vdots \\ \sin(x_L - y_{L,\tau}) \end{pmatrix}. \tag{12}$$

### 3 Examples

In the following examples, we apply the method to several oscillatory systems. In general, oscillation is not required for the method to work, however oscillatory systems are of particular importance for a range of tasks including industrial human-machine interactions.

#### 3.1 Harmonic oscillatory source

We consider a slave that anticipates a harmonic oscillating source such that the evolution equations are given by

$$\begin{aligned} \frac{d}{dt} x &= \omega \\ \frac{d}{dt} y &= \omega + k \sin(x - y_\tau) + \sqrt{Q} \Gamma(t) \end{aligned} \tag{13}$$

where  $x(t), y(t) \in [0, 2\pi]$  are the running phase of master and slave, respectively.

Such a system may reflect an experimental situation in which participants are asked to track a harmonic oscillating target by maintaining zero relative phase, see Figure 3. In this setup, there is a delay induced between a participant's motion and the effect of that motion on the screen. This delay makes it necessary that the participants anticipate the master signal in order to synchronize with it. A simulation of equation (13) is shown in Figure 4. As is evident in the figure, the slave system has synchronized with the future of the master system.

As mentioned in the introduction we expect that the variances in general decrease as a function of  $k$  and increase with  $Q$ . In order to study the dependency of the variance on  $k$  and  $Q$  for illustrative purposes we prefer to replace  $k$  with  $1/k$ . Then, we expect that the variance is a monotonically increasing function of both parameters  $1/k$  and  $Q$ . The variance of the synchronization error as a function  $1/k$  and  $Q$  for a fixed delay  $\tau$  is shown in Figure 5.

In order to evaluate the method's performance, equation (13) is simulated at several values of  $k$  and  $Q$ . For

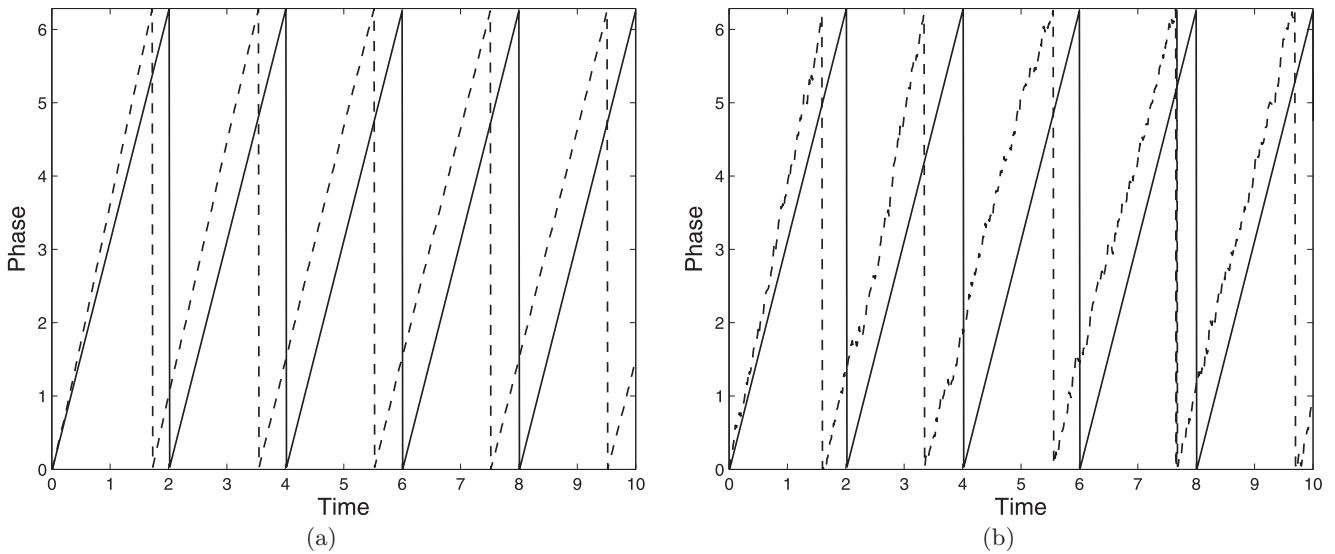


**Fig. 4.** Simulation of a harmonically oscillating master (solid) and slave (dashed) in (a) low and (b) high noise conditions. For the low noise condition,  $Q = 0.1$ , otherwise  $Q = 20$ .

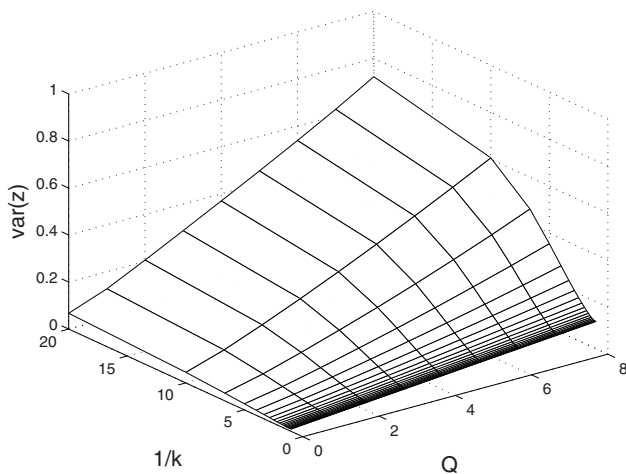


**Fig. 5.** Variance of the synchronization error  $e(t) = y(t - \tau) - x(t)$  as a function of  $1/k$  and  $Q$ .

each resulting time series, the method results in a pair of  $k$  and  $Q$  estimates. These estimates are summarized in Figure 6.

The plots show that estimates of  $k$  vary directly with the simulated values, while having no appreciable dependence on  $Q$ . Similarly, estimates of  $Q$  vary directly with simulated values, with no dependence on  $k$ . In short, Figure 6 reveals that the estimated  $k$  and  $Q$  values are approximately equivalent to the original  $k$  and  $Q$  values used to generate the data.

### 3.2 Nonharmonic oscillatory source

If the oscillations of master and slave are non-harmonic, then the running phase will increase nonlinearly as a func-

tion of time. Let us consider a system in which the phase dynamics slows down close to 0 and 180 degrees and speeds up at 90 and  $-90$  degrees. A master-slave system exhibiting such as behavior is defined by

$$\frac{d}{dt}x = \omega - \delta \sin(2x) \quad (14)$$

$$\frac{d}{dt}y = \omega - \delta \sin(2y) + k \sin(x - y_\tau) + \sqrt{Q}\Gamma(t)$$

with  $\delta > 0$ . A simulation of this model is shown in Figure 7. The variance of the synchronization error as a function of the parameter  $1/k$  and  $Q$  is shown in Figure 8. Again, the slave has synchronized with the master such that it maintains a negative relative phase relationship.

We applied the data analysis method to computer generated data sets. The results, shown in Figure 9, again show that estimates of  $k$  and  $Q$  agree with simulated values, while lacking dependence on one another.

### 3.3 Chaotic systems

The oscillation of the master and slave may go beyond being merely non-harmonic; oscillations may be chaotic as well. A standard chaotic oscillator we may consider is the Rössler system [18]

$$\frac{d}{dt}x_1 = -x_2 - x_3$$

$$\frac{d}{dt}x_2 = x_1 + ax_2$$

$$\frac{d}{dt}x_3 = b + x_3(x_1 - c). \quad (15)$$

In order to simplify notation, let  $f_R(x)$  denote the function mapping the 3-dimensional state vector  $x$  to equation (15).

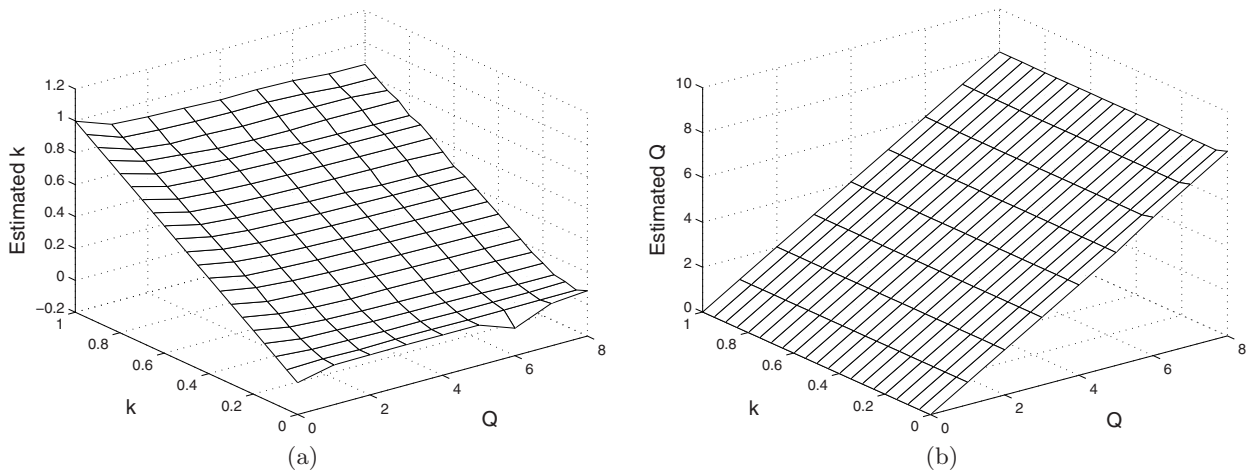


**Fig. 6.** Parameters  $k$  (left panel) and  $Q$  (right panel). Reconstructions versus originals for several parameters delays  $\tau$ .

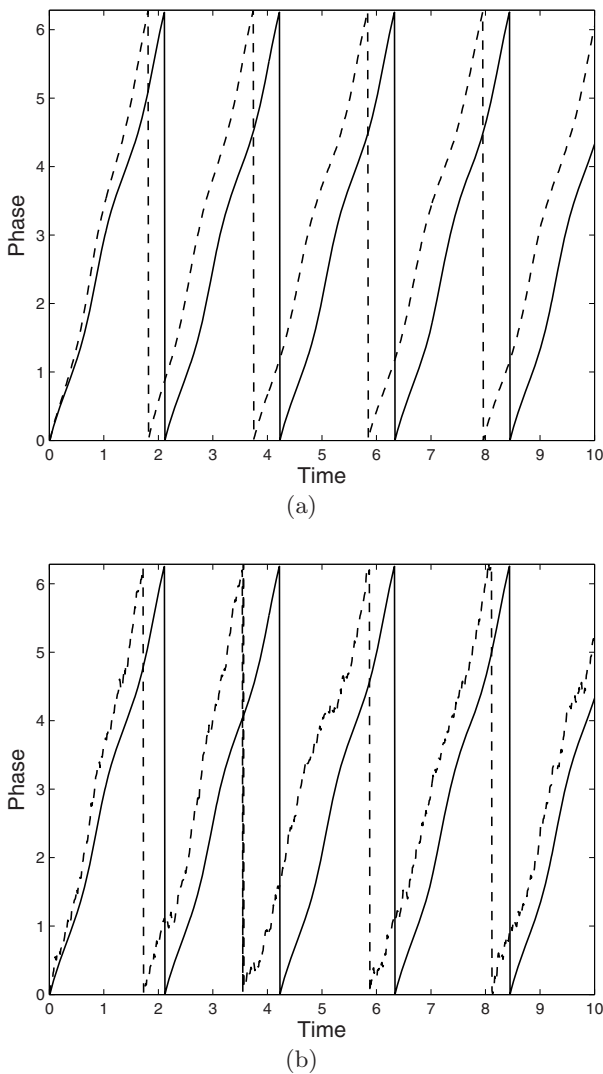


**Fig. 7.** Simulation of a nonharmonically oscillating master (solid) and slave (dashed) in (a) low and (b) high noise conditions. For the low noise condition,  $Q = 0.1$ , otherwise  $Q = 20$ .

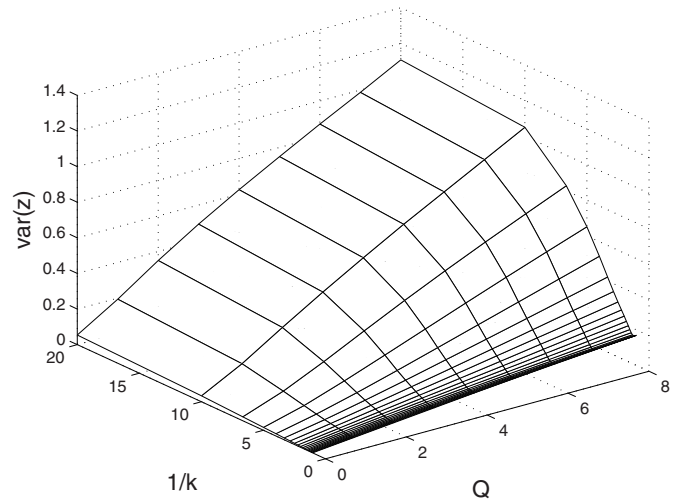


**Fig. 8.** Variance of the synchronization error  $e(t) = y(t - \tau) - x(t)$  as a function of  $1/k$  and  $Q$ .

In this way, we may retain familiar notation defining the master-slave system

$$\begin{aligned} \frac{d}{dt}x &= f_R(x) \\ \frac{d}{dt}y &= f_R(y) + k(x - y_\tau) + \sqrt{Q}\Gamma, \end{aligned} \tag{16}$$

where  $k$  is an appropriate coupling matrix.

A simulation of this model is shown in Figure 10. The variance of the synchronization error as a function of the parameters  $k$  and  $Q$  is shown in Figure 11.

We applied the data analysis method to computer generated data sets. The results are shown in Figure 12. Interestingly, the variability of a chaotic time series works to the method's advantage. Again, the estimate of  $k$  shows no dependence on  $Q$ , but near perfect correspondence to  $k$ .

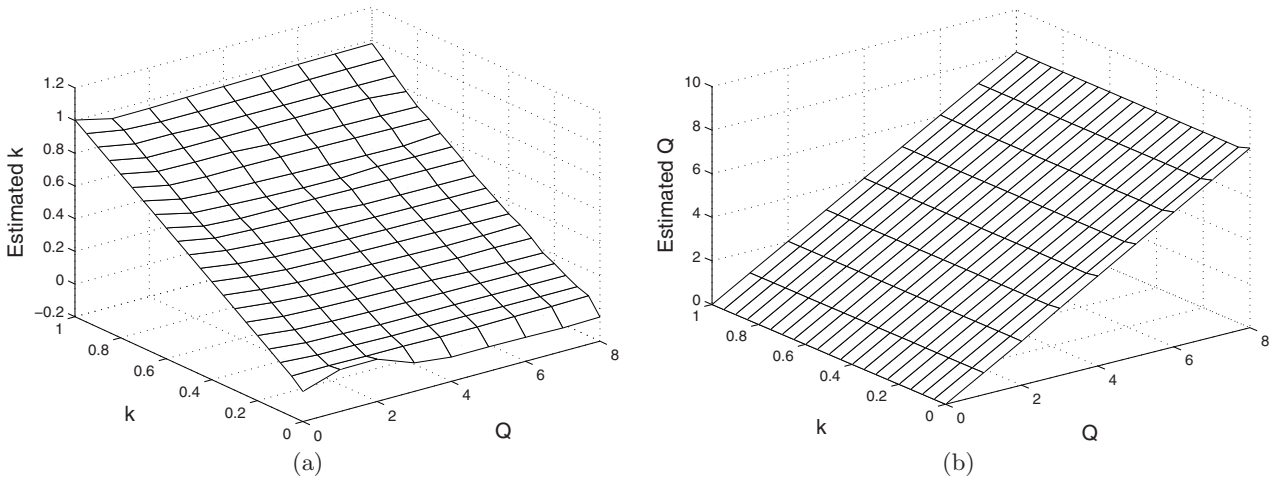


**Fig. 9.** Parameters  $k$  (left panel) and  $Q$  (right panel). Reconstructions versus originals for several parameters  $\delta$ .

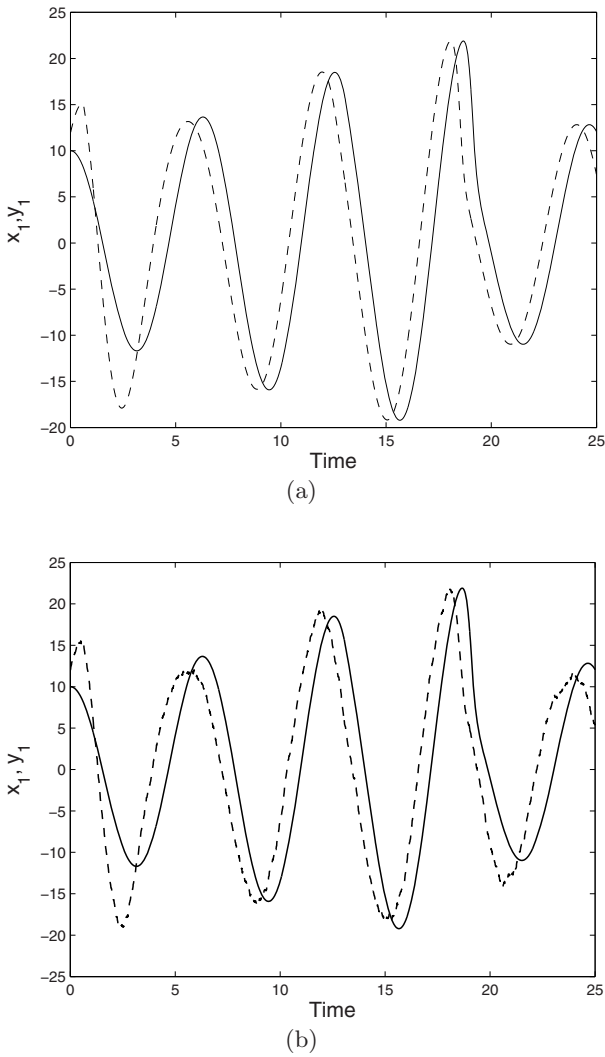


**Fig. 10.** Simulation of a chaotically oscillating master (solid) and slave (dashed) in (a) low and (b) high noise conditions. For the low noise condition,  $Q = 0.1$ , otherwise  $Q = 20$ .

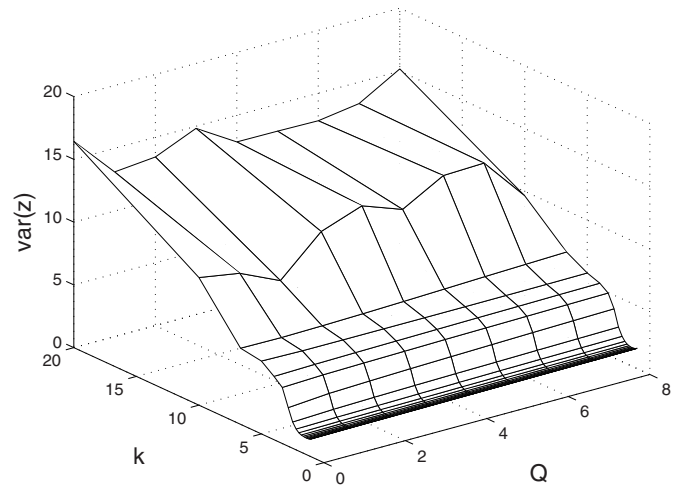


**Fig. 11.** Variance of the synchronization error  $e(t) = y(t - \tau) - x(t)$  as a function of  $1/k$  and  $Q$ .

Likewise, the estimate of  $Q$  is independent of  $k$ , but corresponds to  $Q$ .

### 4 Conclusions

The method developed above allows characterization of experimental data in cases where components can be described as equation (2). This situation obtains, for instance, whenever one system (so-called slave) is following a signal while overcoming some delay. This situation is exemplified in Figure 3. We expect that error in synchronization is a window into the dynamical particulars of the system which has produced a particular time series. Specifically, synchronization error depends on the coupling between slave and master on the one hand, and the coupling of slave to noise sources on the other. Therefore, we only arrive at an understanding of synchronization error

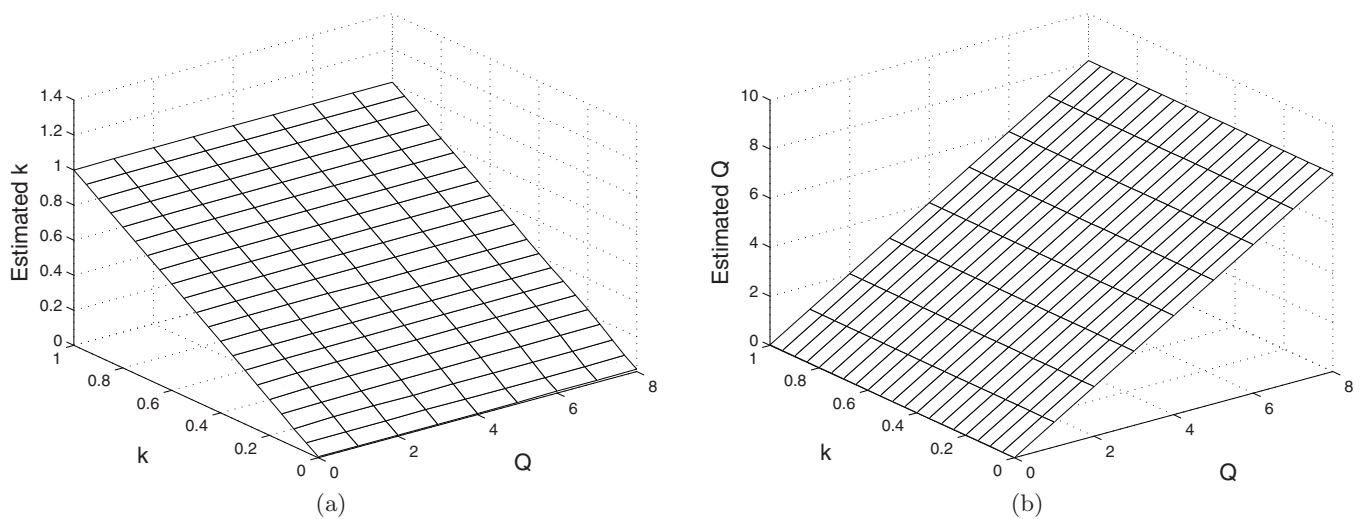


**Fig. 12.** Parameters  $k$  (left panel) and  $Q$  (right panel). Reconstructions versus originals for several parameters  $\delta$ .

if we have estimates of the respective coupling parameters at our disposal. The method above provides a way to estimate these parameters.

Our method, however, requires a priori knowledge of the dynamics of the slave system in question. When difficult to model systems, e.g. human subjects, are involved this is not an optimal situation. If the slave system can be, at least roughly, modelled as a second order differential equation of the form

$$\begin{aligned} \frac{d}{dt}y_1 &= y_2 \\ \frac{d}{dt}y_2 &= h(y_1) \end{aligned} \quad (17)$$

then the function  $h$  can be estimated with relatively little effort.

The useful feature of these systems is that  $dy_1/dt$  is always the same, namely  $y_2$ . Given a time series of  $y_1$  for the slave, we can recover  $y_2$  by simply taking the derivative. From here, the method follows as before. Systems of this form span many oscillatory systems which might be of interest. If  $h(y_1) = -y_1$ , for instance, we have a simple harmonic oscillator, but  $h$  may be arbitrarily complicated.

Therefore, the assumption stays the same, but in a great many cases we may make the assumption small. It is left to be investigated how far this assumption may be pushed. That is, given a slave system which *cannot* be modeled as equation (17), to what extent are the results corrupted by approximating it as so.

This particular arrangement appears to apply well to the exemplar experiment depicted in Figure 3. In this case, the master is known completely, since it is generated. The participant, in general, has unknown dynamics. There is experimental evidence, however, that the dynamics of human coordination are approximated by some second order differential equation [19–21].

## References

1. A. Pikovsky, M. Rosenblum, J. Kurths, R. Hilborn, *Synchronization: A Universal Concept in Nonlinear Science* (Cambridge Univ. Press, 2003)
2. T. Sheridan, W. Ferrell, *Man-machine systems: information, control, and decision models of human performance* (MIT Press, 1974)
3. C. Wickens, *Engineering psychology and human performance*, 2nd edn. (Harper-Collins, New York, 1992)
4. A. Budini, M. Cáceres, *Physica A* **387**, 4483 (2008)
5. G.R. Jafari, S.M. Fazeli, F. Ghasemi, S.M.V. Allaei, M.R.R. Tabar, A.I. Zad, G. Kavei, *Phys. Rev. Lett.* **91**, 226101 (2002)
6. P. Sura, J. Barsugli, *Phys. Lett. A* **305**, 304 (2002)
7. M. Waechter, F. Riess, T. Schimmel, U. Wendt, J. Peinke, *Eur. Phys. J. B* **41**, 259 (2004)
8. T. Kuusela, *Phys. Rev. E* **69**, 031916 (2004)
9. T.D. Frank, P.J. Beek, R. Friedrich, *Phys. Lett. A* **328**, 219 (2004)
10. R. Friedrich, J. Peinke, *Phys. Rev. Lett.* **78**, 863 (1997)
11. J. Gradisek, R. Friedrich, E. Govekar, I. Grabec, *Phys. Lett. A* **294**, 234 (2002)
12. A. Wilmer, T.D. Frank, P.J. Beek, R. Friedrich, *Eur. Phys. J. B* **60**, 203 (2007)
13. H.U. Voss, *Phys. Rev. E* **61**, 5115 (2000)
14. H.U. Voss, *Phys. Rev. Lett.* **87**, 014102 (2001)
15. M. Cizak, F. Marino, R. Toral, S. Balle, *Phys. Rev. Lett.* **93**, 114102 (2004)
16. S. Sivaprakasam, E.M. Shahverdiev, P.S. Spencer, K.A. Shore, *Phys. Rev. Lett.* **87**, 154101 (2001)
17. M.G. Rosenblum, A.S. Pikovsky, J. Kurths, *Phys. Rev. Lett.* **78**, 4193 (1997)
18. O. RöSSLer, *Phys. Lett. A* **57**, 397 (1976)
19. B. Kay, J. Kelso, E. Saltzman, G. Schönner, *J. Experimental Psychology: Human Perception and Performance* **13**, 178 (1987)
20. D. Mottet, R. Bootsma, *Biol. Cybern.* **80**, 235 (1999)
21. P. Silva, M. Moreno, M. Mancini, S. Fonseca, M.T. Turvey, *Neurosci. Lett.* **429**, 64 (2007)